VALIDATION OF A NUMERICAL SIMULATION OF THE COMBUSTION OF NATURAL GAS IN A CYLINDRICAL CHAMBER

Cristiano V. da Silva.
Department of Mechanical Engineering – UFRGS. Rua Sarmento Leite, 425, 90050-170 - Porto Alegre, RS, Brazil.
cristiano@mecanica.ufrgs.br

Horácio A. Vielmo.
Department of Mechanical Engineering – UFRGS. Rua Sarmento Leite, 425, 90050-170 - Porto Alegre, RS, Brazil.
vielmoh@mecanica.ufrgs.br

Francis H. R. França.
Department of Mechanical Engineering – UFRGS. Rua Sarmento Leite, 425, 90050-170 - Porto Alegre, RS, Brazil.
frfranca@mecanica.ufrgs.br

Summary. *This work presents the results of a numerical simulation of the combustion of natural gas and atmospheric air in an axissymmetrical cylindrical chamber. The simulations is performed assuming staged non pre-mixture combustion process in two global steps, where the fuel is injected through a central circular duct, and air is injected through an annular external duct, both in the same plane. The mass, momentum, energy and chemical species conservation equations are solved. Thermal radiation in the interior of the chamber is modeled by the zonal method, in which the wavelength dependence of the gas properties is resolved by the Weighted-Sum-of-Gray-Gases-Model (WSGGM). Turbulent flow is described by the $k-\varepsilon$ model. For the chemical reactions, the Eddy Breakup-Arrhenius model is employed. The resulting differential governing equations are solved by the Control Volume approach. The results include all the flow regions, the chemical species distributions, the velocity fields and the net heat transfer by radiation.*

Keywords. *Combustion, $k-\varepsilon$, Eddy Breakup - Arrhenius, Zonal Method, WSGGM, Finite Volumes.*

1. Introduction

The usual modeling of the combustion process in chamber is based on the mass, energy, chemical species and momentum conservation equations, coupled to turbulence models such as $k-\varepsilon$ (Launder and Sharma, 1974), as can be found in Eaton et al. (1999). A number of approaches based on the Arrhenius rules (Kuo, 1986; Fluent, 1997), Magnussen models, Eddy Breakup model (Magnussen and Hjertager, 1976; Kuo, 1986; Turns 2000), as well as the radiative heat transfer models based on the radiative transfer equations (Siegel and Howell, 2002), have been presented. Among the employed combustion models, one can find the generalized finite-rate models, such as the E-A (Eddy Breakup – Arrhenius) and the so called Probability Density Functions (Kuo, 1986; Fluent, 1997). Nieckele et al. (2001) carried on a numerical study on a combustion process in a cylindrical chamber, burning natural gas, in which the radiation heat transfer was modeled by the Discrete Transfer Model (Carvalho et al., 1991; Fluent, 1997). The gas absorption coefficient dependence on the wavelength was modeled by the Weighted-Sum-of-Gray-Gases-Model (Smith et al. 1982). In this work, the E-A, β-PDF, Arrhenius and Eddy-Breakup models were employed. In the comparison with the experimental data by Magel et al. (1996), it was shown that the E-A model was the one that presented the best agreement. In a following work, Nieckele et al. (2002) proposed a numerical study of the same chamber, employing again the E-A model, but considering two combustions process situations. In the first one, it was employed a single-step global reaction to predict the fuel burning; in the second situation, two-step reaction was assumed. The results were also compared to the experimental data of Magel et al. (1996), achieving a good agreement for both situations, but the second one presented better overall agreement. Zhou et al. (2002) presented a numerical simulation of the formation of NOx in turbulent combustion processes using the Unifield Second-Order Moment chemical reactions model. This model is based on the Navier-Stokes equations, the $k-\varepsilon$ turbulence model, the energy and chemical species conservation equations, as well as the equations of finite rates of chemical reactions based on the Arrhenius' law. The control volume scheme was employed for discretization of the equations. The results were compared to experimental data as well as other combustion models, such as the E-A and the pre-PDF models, achieving a good agreement. da Silva et al. (2004) performed the validation of a model for non staged turbulent combustion processes, without pre-mixture, of methane and atmospheric air. The employed combustion model was Simple-Chemical Reactions Systems (SCRS) proposed by Spalding (1979). In this work, the radiative heat transfer was modeled by the zonal approach, assuming an absorption coefficient of 0,5 m^{-1}. The obtained results were compared to experimental data available in the literature. Due to the complexity of the problem, it was found that the model could be used only in fast estimations, but greater precision would require more sophisticated combustion models.

The present work presents a numerical simulation of staged combustion process of fuel and air, without pre-mixture, in a cylindrical chamber, using the same conditions of the experiments by Garréton and Simonin (1994) for comparison purpose. The E-A model (Eddy Breakup – Arrhenius) was used to find the rate of oxidation of the chemical species. The thermal radiation was accounted by the Zonal Method.

2. Mathematical formulation

It is considered that the combustion process occurs at finite rates, in which the oxidation reaction of the methane involves two global steps:

$$2CH_4^{(16)} + 3\left(O_2^{(32)} + 3,76N_2^{(28)}\right) \rightarrow 2CO^{(28)} + 4H_2O^{(18)} + 11,28N_2^{(28)}$$
$$2CO^{(28)} + 1\left(O_2^{(32)} + 3,76N_2^{(28)}\right) \rightarrow 2CO_2^{(44)} + 3,76N_2^{(28)}$$

(1)
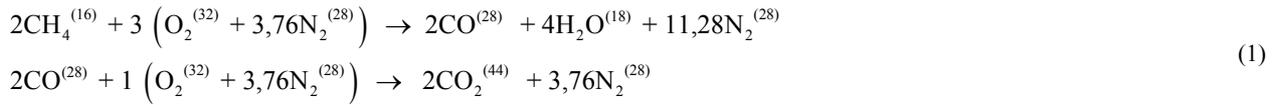
It is assumed that the heat transfer have already reached steady state. Based on the knowledge that the heat transfer rate occurs from the high temperature gases (combustion products) to the chamber outside, the focus of the present work is analyzing the behavior of the process with respect to the heat transfer, the mixture components concentrations and the characteristics of the flame in the combustion chamber. The problem can be stated as: for a given chamber geometry, compute the temperature and the chemical species concentration distributions to validate the proposed formulation. The time-averaged equations were adopted, in which the turbulent flow is described by the $k-\varepsilon$ model. Thermal radiation is evaluated by the Zonal Method, where the direct-exchange areas between the gas and surface zones are determined by the relations presented by Sika (1991), and the WSGGM is used to account the absorption coefficient wavelength dependence. The coefficients and weights of the model are taken from Smith et al. (1981) for uniform concentrations of 20% of H_2O, 10% of CO_2 and 70% of N_2.

2.1 Mass conservation

Adopting cylindrical coordinates and assuming axissymmetry, one obtains:

$$\frac{\partial}{\partial x}\left(\rho\overline{u}\right) + \frac{\partial}{\partial r}\left(\rho\overline{v}\right) + \frac{\rho\overline{v}}{r} = 0$$

(2)

in which x and r are the radial and the axial coordinates, $\overline{u}$ and $\overline{v}$ are the average velocities in the respective directions, and ρ is the density. The bars over some terms indicate Reynolds Average.

2.2 Momentum equations in the axial ($\overline{u}$) and radial ($\overline{u}$) directions

$$\overline{u}\frac{\partial}{\partial x}\left(\rho\overline{u}\right) + \overline{v}\frac{\partial}{\partial r}\left(\rho\overline{u}\right) = -\frac{\partial p^*}{\partial x} + \vec{\nabla}\bullet\left(\left(\mu+\mu_t\right)\vec{\nabla}\overline{u}\right) + \frac{\partial}{\partial x}\left(\mu_t\frac{\partial\overline{u}}{\partial x}\right) + \frac{1}{r}\frac{\partial}{\partial r}\left(r\mu_t\frac{\partial\overline{v}}{\partial x}\right)$$

(3)

$$\overline{u}\frac{\partial}{\partial x}\left(\rho\overline{v}\right) + \overline{v}\frac{\partial}{\partial r}\left(\rho\overline{v}\right) = -\frac{\partial p^*}{\partial r} + \vec{\nabla}\bullet\left(\left(\mu+\mu_t\right)\vec{\nabla}\overline{v}\right) + \frac{\partial}{\partial x}\left(r\mu_t\frac{\partial\overline{u}}{\partial r}\right) + \frac{1}{r}\frac{\partial}{\partial r}\left(r\mu_t\frac{\partial\overline{v}}{\partial r}\right) - \frac{\left(\mu+\mu_t\right)\overline{v}}{r^2} + \frac{\rho\overline{w}^2}{r}$$

(4)

where μ is the dynamic viscosity, μ_t is turbulent viscosity, computed from the standard $k-\varepsilon$ model by $\mu_t = C_\mu\rho k^2/\varepsilon$, $p^* = \overline{p} - (2/3)k$ represents the modified pressure, C_μ is an empirical turbulence model, $\overline{p}$ is the average pressure, k and ε are the turbulent kinetic energy and its dissipation, respectively.

2.3 "Eddy Breakup - Arrhenius" (E-A) chemical reactions model

2.3.1. Chemical-species conservation

The reduced model of chemical reactions that is employed here assumes finite-rate chemical reactions, at steady state. In addition, it is considered that the fuel oxidation is staged, involving two global steps without pre-mixture. Six chemical species are present in the mixture: oxygen, methane, nitrogen, water vapor and carbon monoxide. A conservation equation is required for all the components, except for the nitrogen. In this way, assuming a Lewis number of 1.0, one obtains the following conservation equation of the α–th chemical species:

$$\overline{u}\frac{\partial}{\partial x}\left(\rho\overline{f_\alpha}\right) + \overline{v}\frac{\partial}{\partial r}\left(\rho\overline{f_\alpha}\right) = \vec{\nabla}\bullet\left(\left(\rho D + \frac{\mu_t}{Sc_t}\right)\vec{\nabla}\overline{f_\alpha}\right) + \overline{R_\alpha}$$

(5)

where D is the mass diffusivity, Sc_t is the Schmidt number, $\overline{f_\alpha}$ is the average mass fraction of the α–th chemical species of the mixture, and $\overline{R_\alpha}$ is the average volumetric rate of the formation or destruction of the α–th chemical species. This term is computed as the summation of all volumetric rates of formation or destruction in all chemical reactions k in which α is present, $\overline{R_{\alpha,k}}$. Thus, one finds that $\overline{R_\alpha} = \sum_k \overline{R_{\alpha,k}}$, and this rate of formation or destruction, $\overline{R_{\alpha,k}}$, can be obtained by an Arrhenius kinetic rate relation or by relations that consider the influence of turbulence, such as the Magnussen's equation

(Eddy Breakup) (Magnussen and Hjertager, 1976), or also by both ways (Eaton et al., 1999; Fluent, 1997). The equation of Arrhenius, assuming average temperature and concentrations, can be written as:

$$\overline{R_{\alpha,k}} = -\eta_{\alpha,k}\overline{MM}_\alpha \overline{T}^{\beta_k} A_k \Pi_{\alpha_{reagentes}}\overline{C_\alpha}^{\gamma_{\alpha,k}} exp\left(\frac{-E_k}{\overline{R}\overline{T}}\right) \tag{6}$$

where β_k is the temperature exponent of each reaction k, which is obtained empirically, together with the activation energy E_k, and the coefficient A_k. In the above equation, Π_α is the product symbol, $\overline{C_\alpha}$ is the average molar concentration for each reacting species α, $\gamma_{\alpha,k}$ is the concentration exponent for each reacting component α in reaction k, $\overline{R}$ is the universal ideal gas constant, $\overline{MM}_\alpha$ and $\eta_{\alpha,k}$ are the molecular mass and the stoichiometric coefficient of the α-th chemical species that are present in the k-reactions.

In the Eddy-Breakup model, the chemical reaction rates of the species are based on the theories of vortices dissipations in the presence of turbulence. In this way, the average rate of the chemical reactions for the α-th reacting chemical species, in the k-th reaction, to represent both diffusive and non pre-mixture turbulent flames can be found between the smallest value (that is, the limit rate) between the following equations:

$$\overline{R_{\alpha,k}} = -\eta_{\alpha,k}\overline{MM}_\alpha K_1 K_2 \rho \frac{\varepsilon}{k}\frac{\overline{f_{\alpha^*}}}{\eta_{\alpha^*,k}\overline{MM}_{\alpha^*}} \qquad \text{and} \qquad \overline{R_{\alpha,k}} = \eta_{\alpha,k}\overline{MM}_\alpha K_1 K_2 \rho \frac{\varepsilon}{k}\frac{\sum_p\overline{f_p}}{\sum_p\eta_{p,k}\overline{MM}_p} \tag{7}$$

where the sub-index α^* represents the α-reacting component that leads to the smallest value for $\overline{R_{\alpha,k}}$, and the sub-index p represents the combustion gas products. In the above equations, K_1 and K_2 are empirical constants having the value of 4 and 0.5 (Magnussen and Hjertager, 1976). Finally, for the Arrhenius-Magnussen combined model (Eqs. (6) and (7)), the final value of the rate of formation or destruction of the chemical species, which must be employed in the calculation of the source terms of the energy and chemical species conservation equations, is taken as the smallest value between the values obtained in the two models.

2.3.2 Energy conservation

For the energy transport due to the flow inside the chamber, neglecting the energy transport due to the diffusion of each species ($Le = 1$), one finds:

$$\overline{u}\frac{\partial}{\partial x}\left(\rho\overline{h}\right)+\overline{v}\frac{\partial}{\partial r}\left(\rho\overline{h}\right)=\overline{\nabla}\cdot\left(\left(\frac{\kappa}{c_p}+\frac{\mu_t}{Pr_t}\right)\overline{\nabla}\overline{h}\right)+\overline{S}_{rad}+\sum_\alpha\left[\frac{h_\alpha^0}{\overline{MM}_\alpha}+\int_{\overline{T}_{ref,\alpha}}^{\overline{T}}c_{p,\alpha}d\overline{T}\right]\overline{R_\alpha} \tag{8}$$

where $\overline{h} = \int c_p d\overline{T}$ is the average enthalpy of the mixture and c_p is the specific heat, defined as $c_p = \sum_\alpha\overline{f_\alpha}c_{p,\alpha}$, where $c_{p,\alpha}$ is the specific heat of the α-th chemical species, $\overline{T}$ is the average temperature, κ is the thermal conductivity of the mixture, Pr_t is the turbulent Prandtl number, $\overline{S}_{rad}$ is the source term due to the heat transfer by radiation, h_α^0 and $\overline{T}_{ref,\alpha}$ terms are the enthalpy of formation and the reference temperature of the α-th chemical species. Completing the model, the mixture-density can be found from the ideal gas state equation (Kuo, 1986, Fluent, 1997, Turns, 2000), $\rho = p\overline{MM}\left(\overline{R}\overline{T}\right)^{-1}$, where p is the chamber operational pressure, which in this equations is taken as 1.0 atm (Spalding, 1979) and $\overline{MM}$ is the mixture molecular mass. All the equations here presented are valid only for the turbulent core, where $\mu_t >> \mu$. Next to the walls, the law of the wall, recommended by Freire et al. (2002), is used. The law of the wall is obtained assuming turbulent equilibrium in the regions close to the solid surfaces, and must be applied in the region between the surface and the first simulation nodal point. This law consists of prescribing a logarithmic velocity profile in the turbulent region, and a linear profile in the laminar sub-layer. This way, for $y^+ \leq 11,5 \to u^+ = y^+$ and for $y^+ > 11,5 \to u^+ = (1/A)\ln(y^+) + \Psi$, where $y^+ = y\left(\rho C_\mu^{1/4}k^{1/2}\mu^{-1}\right)$ is the dimensionless distance to the wall, $u^+ = \overline{u}/u^*$ is the dimensionless velocity, $u^* = \sqrt{\tau_w/\rho}$ is the friction velocity, where τ_w is the shear stress in the wall and y is the distance from the wall. According to Nikuradse (1933), $A = 0.4$ and $\Psi = 5.5$. From the assumption of equilibrium between the production and destruction of turbulent kinetic energy, and also considering that the shear stress in the wall is approximately constant in this region, it is imposed that the kinetic energy gradient in the wall is null. In the wall, $\varepsilon = C_\mu^{3/4}k^{3/2}\left(Ay\right)^{-1}$. For the determination of the source term due to thermal radiation that is present in the combustion process, the Zonal Method (Siegel and Howell, 2002) is employed, which is based on the division of the domain into gas and surface zones, whose temperatures can be assumed uniform. Since the presence of soot in gas combustion is negligible, it can be assumed with a good precision that the medium does not scatter thermal radiation. The dependence of the

absorption coefficient is based on the Weighted-Sum-of-Gray-Gases-Model (WSGGM). Applying a balance of radiative energy in each gas zone per unit of volume (W/m³), one finds:

$$\overline{S}_{rad,\gamma} = -\frac{1}{V_\gamma}\left(\sum_i 4V_\gamma a_i \sigma \overline{T}_\gamma^4 - \sum_{\gamma^*=1}^{\Gamma} \overrightarrow{g_{\gamma^*}g_\gamma} \sigma \overline{T}_{\gamma^*}^4 - \sum_{j=1}^{J} \overrightarrow{s_j g_\gamma} q_{o,j}\right) \tag{9}$$

On the right-side, the first term in the parentheses represents the amount of the thermal radiation emitted by the gas zone V_γ, the second and the third term accounts for the radiation energies absorbed by the gas zone V_γ that are originated from the other gas zones V_{γ^*} and the other surface zones j. The term σ represents the Stefan-Boltzmann constant, $\overrightarrow{g_{\gamma^*}g_\gamma}$ and $\overrightarrow{s_j g_\gamma}$ are the gas-to-gas and the surface-to-gas directed-flux areas. Repeating the procedure for the surface zone A_k, one finds the net radiative heat flux (in W/m²) as:

$$\overline{S}_{rad,k} = \frac{1}{A_k}\left(\sum_{\gamma=1}^{\Gamma} \overrightarrow{g_\gamma s_k} \sigma \overline{T}_\gamma^4 + \sum_{j=1}^{J} \overrightarrow{s_j s_k} q_{o,j}\right) - q_{o,k} \tag{10}$$

where, in the right-hand side, the first term in the parentheses represents the radiation energy emitted by the gas zone V_γ that reaches surface zone k, the second term is the radiation energy that leaves surface zone j that reaches zone k, and the term $q_{o,k}$ is the outgoing heat flux (radiosity) on surface k. $\overrightarrow{g_\gamma s_k}$ and $\overrightarrow{s_j s_k}$ are the gas-to-surface and surface-to-surface directed-flux areas. For the case of cylindrical geometry, as considered here, these areas are computed from the relations presented by Sika (1991).

3. Problem presentation

It is considered the same combustion chamber that is analyzed in the test case described in Garréton and Simonin, (1994) (Fig.1), and also solved by Nieckele et al. (2002). A 400 kW power burner is placed in the chamber symmetry line to provide the required amount of air and natural gas (90 % of methane and 10 % of nitrogen). An excess of 5 % of fuel is used, resulting in a mass flow rate of 0.0125 kg/s with a temperature of 313.15 K; the mass flow rate of air, at the temperature of 323.15 K, is 0.186 kg/s. For these flow rates, the injection velocities of the fuel and air are approximately 7.76 m/s and 36.29 m/s, respectively. The average Reynolds number at the chamber inlet results in 17900. The composition of the inlet air is 23 % of oxygen, 76 % of nitrogen and 1 % of water vapor. Considering axissymmetry, the computation domain is taken as only a fraction of the entire circular cross-section (one radian). The fan and the other external components of the combustion chamber are not included in the computational domain, but they are considered in the solution, since they supply the entrance conditions in the camera. Buoyancy forces are neglected, since the flow is mainly governed by the inertial forces due to the high velocities provided by the burner.
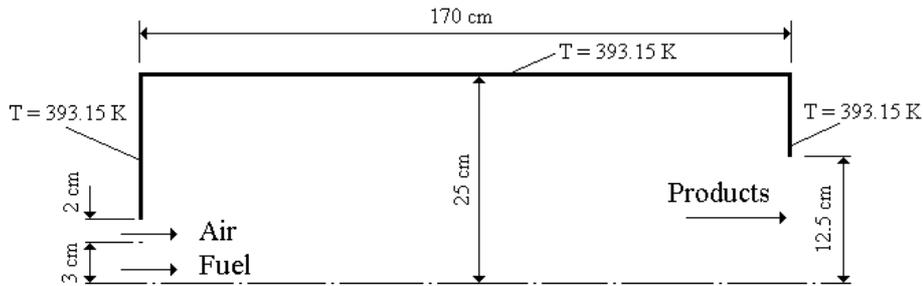

Figure 1. Geometry of the combustion chamber

4. Thermophysical properties

The constants that appear in the Arrhenius equation for the combustion of methane are presented in Tab. 1.

Table 1. Constants of the Arrhenius equation (Turns, 2000; Nieckele et al., 2002)

Step (k)	E_k	A_k	β_k	γ_{CH_4}	γ_{O_2}	γ_{CO}	γ_{CO_2}	γ_{H_2O}
$k=1$	2.03x10⁸	2.8x10¹²	0	-0,3	1.3	-	-	-
$k=2$	1.67x10⁸	2.91x10¹²	0	-	0.25	1	-	-

The constants of the equation and the thermophysical properties of the gases are presented in Tab. 2. Only the specific heats of the gases are considered to be dependent of the temperature, but just to obtain the temperatures in a posterior processing. Their temperature dependences are evaluated with the relations presented in Van Wylen et al. (1998). The specific heat of the mixture was obtained from the mass-fraction weighted average of the specific heats of the species. The mixture transport properties were taken as those of the air, since it is the predominant component of the mixture.

Table 2. Thermophysical properties used in the solution of the problem (from various sources)

Properties	Size	Properties	Size
$\overline{MM}_{N_2}$ (kg/kmol)	28	$\overline{MM}_{CH_4}$ (kg/kmol)	16
$\overline{MM}_{CO_2}$ (kg/kmol)	44	$\overline{MM}_{H_2O}$ (kg/kmol)	18
$\overline{MM}_{CO}$ (kg/kmol)	28	$\overline{MM}_{O_2}$ (kg/kmol)	32
σ (W/m^{2}K^4)	5.6697x10^{-8}	μ (Ns/m^2)	2.97x10^{-5}
κ (W/mK)	45.4x10^{-3}	D (m^2/s)	2.88x10^{-5}
$\overline{R}$ (kJ/kmolK)	8.3145	σ_k (-)	1,0
C_μ (-)	0,09	σ_ε (-)	1.3
$C_{2,\varepsilon}$ (-)	1.92	Sc_t (-)	0.9
$C_{1,\varepsilon}$ (-)	1.44	Pr_t (-)	0.9
$h^0_{CO_2}$ (J/kg)	3.94x10^8	$h^0_{O_2}$ (J/kg)	0
$h^0_{N_2}$ (J/kg)	0	$h^0_{H_2O}$ (J/kg)	2.42x10^8
h^0_{CO} (J/kg)	1.11x10^8	$h^0_{CH_4}$ (J/kg)	7.49x10^7

5. Boundary conditions

Following Garréton and Simonin (1994), it was assumed that the combustion chamber walls were maintained at the temperature of 293.15 K, in addition to the non-slip and impermeability conditions. In the symmetry axis, it was considered that the axial velocity gradient in the radial direction is null. The outlet condition for all variables was null diffusive flux. The axial velocity component, after the outlet of chamber, was corrected by a factor to conserve the mass and avoid counter-flow. In the entire chamber outlet plane the radial velocity component was set null. Wall emissivities were equal to 0.6. The inlet and outlet reservoirs were represented as black surfaces at the temperature of the inlet and outlet gases, respectively. The outlet temperature was computed as $\overline{T}_{bulk} = \left(r\overline{u}c_p\overline{T}\right)\left(r\overline{u}c_p\right)^{-1}$, where $\overline{T}_{bulk}$ was the average temperature of the mixture in the outlet. In the inlet, the flow velocity in the axial direction and the concentration profiles were assumed uniform. The turbulent kinetic energy was taken as $k = \frac{3}{2}\left(\overline{u}_{in}I\right)^2$, where I is the turbulence intensity and $\overline{u}_{in}$ is the inlet axial velocity. For the destruction of the turbulent kinetic energy, it was specified $\varepsilon = C_\mu^{3/4}k^{3/2}/l$, where l is the characteristic length of the turbulence scale. The turbulence intensity at the inlet was prescribed as 6 % for the air and 10 % for the fuel. For the dissipation of the turbulent kinetic energy, it was employed a characteristic length of 0.04 m for the air and 0.03 m for the fuel.

6. Numerical method

The numerical solution of the conservation equations was obtained from the Control Volume method, using the Power-Law to evaluate the fluxes at the boundaries of the control volumes, and the SIMPLE scheme for the $p-v$ coupling. The resulting system of equations was solved by the TDMA scheme, making use of the block correction technique but not for the computation of the turbulent kinetic energy and its dissipation. After grid independence tests, it was found that 30 and 60 volumes in the radial and axial direction led to satisfactorily precise results. Mesh refinement was used in the region close to the symmetry line, where 24 of the 30 volumes in the radial direction are distributed with different spacing in the region of 0 to 12.5 cm, which includes the region occupied by the burner and the exit nozzle. In the region close to the wall, it was also applied a mesh refinement to capture the boundary layer effects. The solution was assumed converged when the summation of the normalized residuals of all the equations were less than 10^{-9}, with exception of the enthalpy residual, which was taken as 10^{-7}.

7. Analysis of the results

Figure 2 presents the gases temperature distribution inside the combustion chamber as obtained in this work. The figure also shows the results presented in Nieckele et al. (2002) for a similar problem for comparison purpose. The latter used the E-A two global steps chemical reaction model, as the present work, but the thermal radiation was evaluated with the DTRM model (Discrete Transfer Radiation Model). It is also shown in the figure the Damköler number distribution, $Da = \left(\tau_t\right)\left(\tau_{ch}\right)^{-1}$, where τ_t and τ_{ch} are the turbulence and the chemical reaction characteristic times, respectively. It can be seen that the magnitude of temperatures presents approximately the same magnitude, with the maximum temperature around 1750 K. Figures 2-a and 2-b show with clarity the jet of cold air and fuel in the center region close to the symmetry line. In this region, the chemical reactions are governed by the Arrhenius chemical kinetics, resulting in a Damköler number less than one. For Figs. 2-a and 2-b, the jets are nearly identical, extending from the inlet up to two-third towards the chamber exit. In this region, there is an intensification of the gas mixture and the start of the combustion fuel, which is first pre-heated and

then experiences a gradual increase of the temperature towards the highest temperatures close to exit region, where the flame is no longer annular and occupies the entire cross section of the chamber. The small difference in the flame shape between the two works are probably due to the different thermal radiation models.


(a)

(b)

(c)
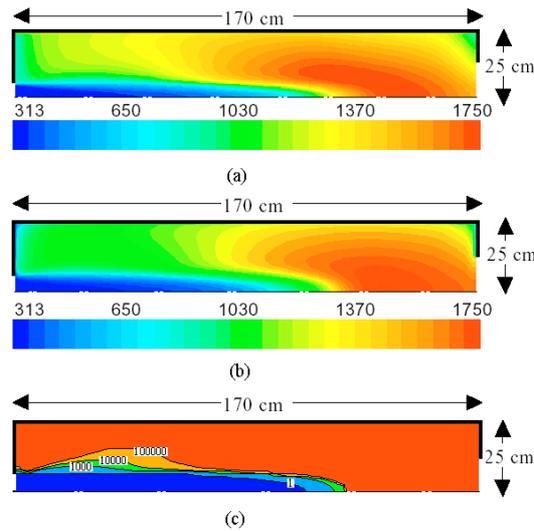
Figure 2. Distribution of temperatures: (a) E-A model with two global steps of chemical reactions - Nieckele et al. (2002); (b) E-A model with two global steps of chemical reactions – present work; (c) Damköler distribution number

In Figure 2-c, it can be observed four regions having equal Damköler number: $Da = 1$, 1×10^3, 1×10^4 and 1×10^5. For Da<<1, the combustion process is governed by the chemical kinetics; for Da>>1, it is governed by the fluid flow mechanics. Thus, it can be verified that the central region, which is occupied by the cold inlet jet, is described by the Arrhenius chemical kinetics, while the other regions are described by the Magnussen's model of instantaneous reactions. Since the chemical kinetics, described by the Arrhenius' equation, is a function of the temperature, the lowest rates of chemical reaction are found in the cold inlet jet. This results in a gradual increase in the temperature, causing pre-heating of the gases, which are more intensely burnt in the posterior part of the chamber due to intensification of the turbulence.

In Fig. 3-a, one can observe that the gases temperature distribution presents a good agreement with the experimental data. The profiles are coincident up to about 1.1 m from the chamber inlet where, for the present work, the combustion process starts, resulting in a steeper increase in the gases temperature. Figure 3-b shows that the obtained fuel concentration (CH_4 mass fraction) profile has a good agreement with the experimental data, following the same trend, although some discrepancy is observed up to 1.1 m from the inlet.


(a)

(b)

(c)
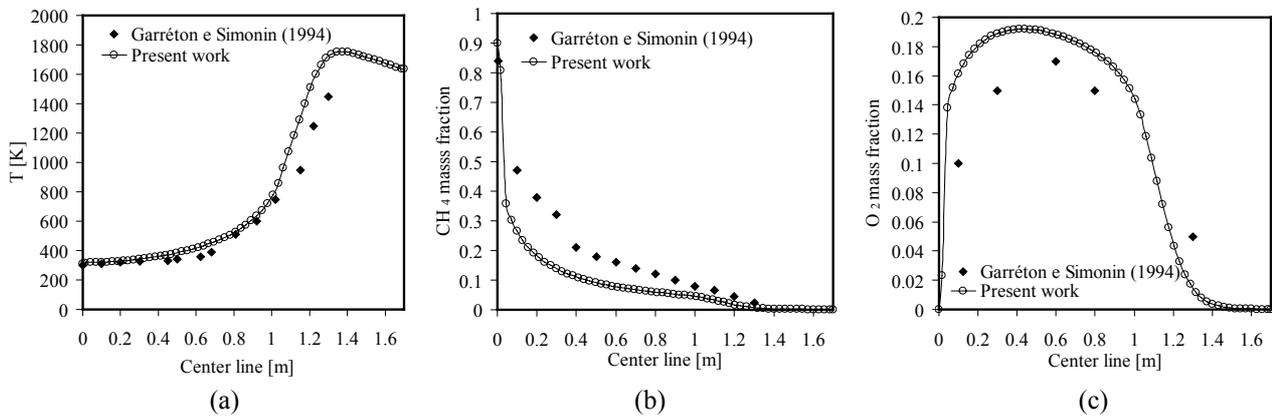
Figure 3. (a) Temperature along the symmetry line; (b) Fuel concentration along the symmetry line; (c) Oxygen concentration along the symmetry line

In this solution, the decrease in the fuel concentration is the greater in the region just after the chamber inlet mostly because of its diffusion, and the following consumption due to chemical reaction in the vicinity of the inlet jet. This can be verified by the greater slope in the fuel concentration profile. In the region of the inlet jet, there is a greater amount of oxygen to react with the fuel that is being injected, intensifying the chemical reaction rate in the region surrounding the jet and leading to a higher consumption. Along the chamber length, the progressive reduction of fuel and oxygen lead to a reduction in the chemical reaction rate. This reduction can be further explained by the verification of the oxygen concentration along the symmetry line, as shown in Fig. 3-c. In this figure, it can also be observed a considerable increase in the oxygen concentration just after the inlet, reaching its peak at about 0.4 m from the inlet, then reducing to extinction. The reduction of the oxygen and fuel concentrations leads to reduction in the rate of chemical reaction in the end of the jet. The increase in the concentration of oxygen along the centerline, shown in Fig. 3-c, is explained by the fact that the air entrance does not take

place in the centerline, but in the annular duct around it. With the start of the combustion process, the concentration of oxygen decreases, leading to an increase in the temperature, as shown in Fig. 3-a, and in the concentration of carbon monoxide (Fig. 4-b), which is formed by the first global reaction that is representative of the combustion process (see Eq. (1)). In Fig. 4-a, it is shown that the concentration of carbon dioxide obtained from the present modeling presents results that are coincident with the experimental data up to 1.1 m from the entrance, from where there is an increase in its concentration. This is related to the increase in the rates of chemical reactions, which also causes an increase in the temperature that is shown in Fig. 3-a in this same region. Figure 3-c shows that the consumption of oxygen becomes a bit higher in this position, for the same reason. In Fig. 4-c, it can be seen that the concentration of carbon monoxide along the radius at 1.312 m from the entrance, albeit being under predicted, shows the same trend of the experimental data. This is also explained by the same explanation involving the CO profile in the centerline.
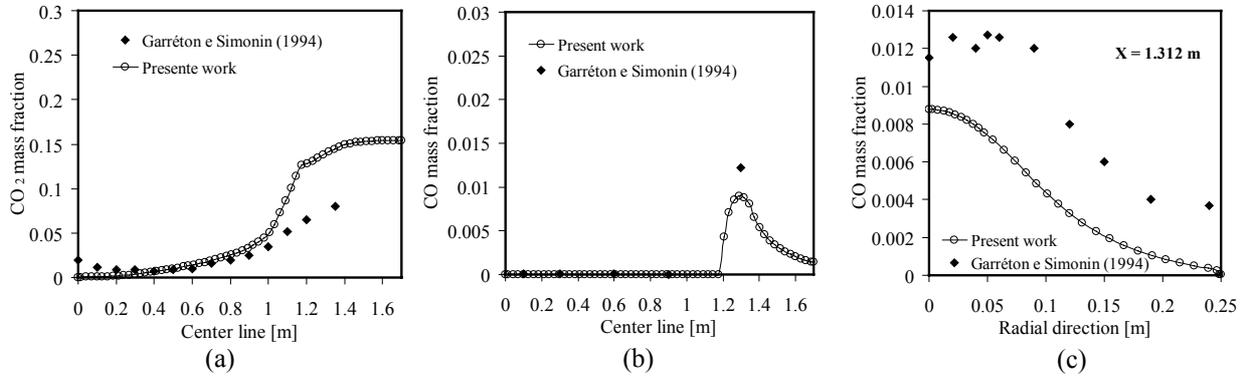

Figure 4. (a) Concentration of carbon dioxide along the symmetry line; (b) Concentration of carbon monoxide along the symmetry line; (c) Concentration of carbon monoxide along the radial position at 1.312 m from the entrance

Figures 5-a to 5-c show a drop in the temperature in the region close to the cylindrical wall of the chamber. This related to the heat transfer to the outside, by means of the prescribed temperature condition of 393.15 K, according to the experiment of Garréton and Simonin (1994). In Fig. 6-b, one observes that the results of the present modeling have the same trend of the experimental data. The discrepancies are related to the model's early prediction of the combustion process, as mentioned before. The same behavior observed at the position of 0.312 m are observed for the position of 0.912 m. Towards the chamber outlet, where the chemical reactions have practically ceased, the magnitude of the temperature results from the gaseous combustion products flow. In Fig. 6 it can be verified that the results obtained for the oxygen concentration follow the same trends of the experimental data at stations 0.312 and 0.912 m. In the regions that are closer to the chamber outlet, position 1.312 m, it is also observed a greater discrepancy in the concentration of oxygen for radial position up to 0.12 m from the centerline. This is also related to the model's early prediction of the combustion process.
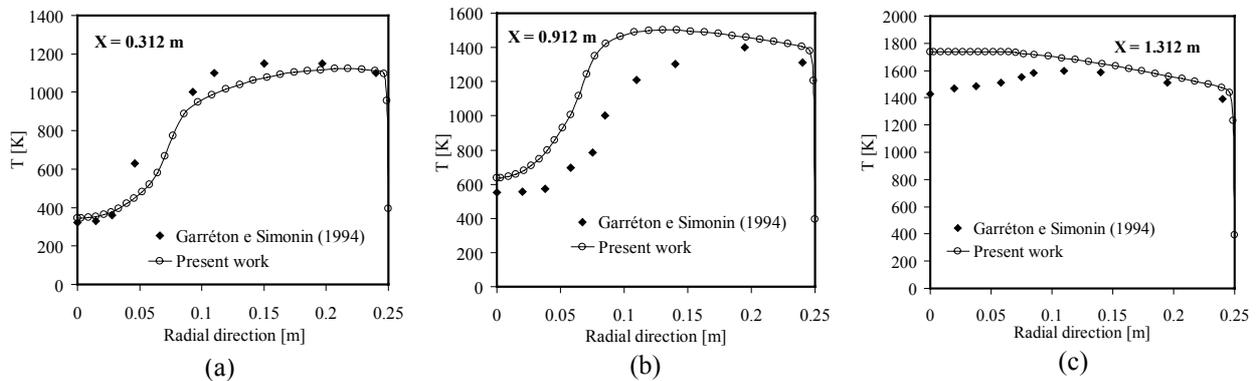

Figure 5. Radial temperature distributions at different distances from the entrance: (a) 0.312 m; (b) 0.912 m ; (c) 1.312 m
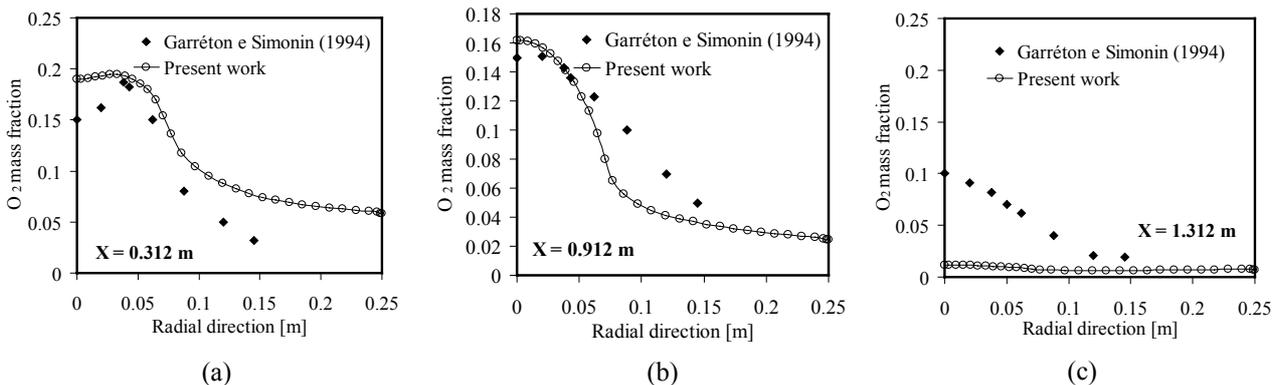
Figure 6. Radial concentration distribution of O_2 at different distances from the inlet: (a) 0.312 m; (b) 0.912 m; (c) 1.312 m

It can be observed in Fig. 7-a that the results for the concentration of CO_2 are satisfactory especially in the regions close to the chamber inlet, for the same reason above mentioned.
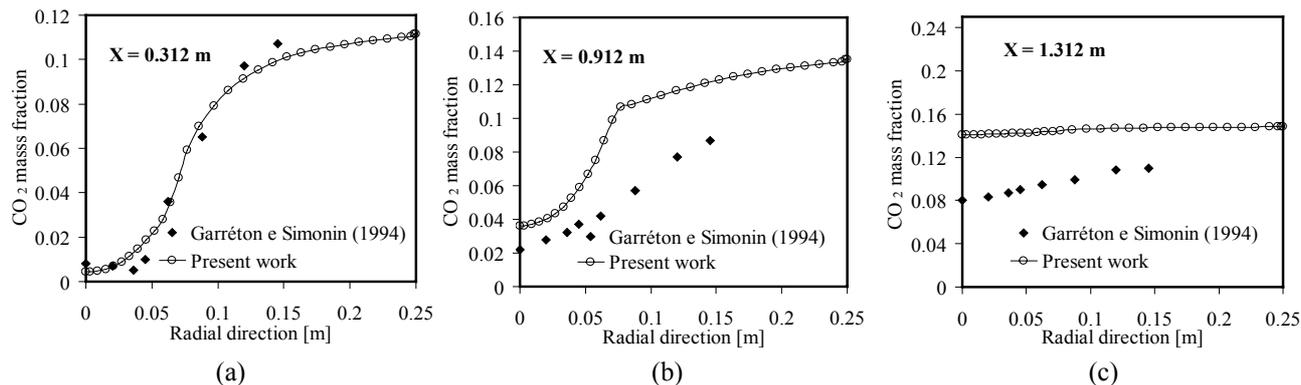

Figure 7. Radial concentration distribution of CO_2 at different distances from the inlet: (a) 0.312 m; (b) 0.912 m; (c) 1.312 m

8. Conclusions

Considering the limitations of the combined Eddy Breakup-Arrhenius model, in general, the present model led to temperature and concentration distributions that satisfactorily match the experimental data, especially in the region up to 1.1 m from the chamber inlet (reactants injection). The results for the CO_2 distribution, both in the symmetry line and along the radius, at 1.313 m from the entrance, were under predicted. The discrepancies between some results, such as the fraction of O_2 e CO_2 close to the chamber exit, were attributed to the behavior of the flame center jet, where a fast pre-heating of the gases increased rapidly the temperature and led to a fast consumption of reactants. This resulted in a higher concentration of CO_2, and a smaller concentration of O_2, in comparison to the experimental data. This is possibly due to the limitations that are present in the proposed methodology, especially with respect to the Eddy Breakup-Arrhenius model.

9. Referências bibliográficas

Carvalho, M.G., Farias, T. and Fontes, P., 1991. "Predicting radiative heat transfer in absorbing, emitting, and scattering media using the discrete transfer method", ASME HTD, Vol. 160, pp.17-26.

da Silva, C. V., Vielmo, H. A. and França, F. H. R, 2004. "Simulação numérica de processos de combustão de gás natural em câmaras cilíndricas usando o modelo SCRS", Proc. of the 10th ENCIT, Rio de Janeiro, Brasil, ABCM.

Eaton, A.M., Smoot, L.D., Hill, S. C. and Eatough, C.N., 1999. "Components, formulations, solutions, evaluations, and application of comprehensive combustion models", Prog. in Energy and Comb. Science, Vol. 25, pp. 387-436.

Fluent (ed.), 1997. "Fluent user's guide", Fluent Incorporated, New Hampshire.

Freire, A.P.S., Menut, P.P.M. and Su, J., 2002. "Turbulência",ABCM, Rio de Janeiro – BR, Vol. 1.

Garréton, D. and Simonin, O., 1994. "Aerodynamics of steady state combustion chambers and furnaces", ASCF Ercoftac CFD Workshop, October 17-18, Org: EDF, Chatou, France.

Kuo, K.K., 1996. "Principles of combustion", John Wiley & Sons, New York.

Launder, B.E. and Sharma, B.I., 1974. "Application of the energy-dissipation model of turbulence to the calculation of flow near a spinning disc", Letters in Heat and Mass Transfer, Vol. 19, pp. 519-524.

Magel, H.C., Schnell, U. and Hein, K.R.G. ,1996. "Modeling of hydrocarbon and nitrogen chemistry in turbulent combustor flows using detailed reactions mechanisms", 3rd Workshop on Modeling of Chemical Reaction Systems.

Magnussen B.F. and Hjertager B. H., 1976. "On mathematical models of turbulent combustion with special emphasis on soot formation and combustion. Proc. of the 16th Int. Symp. on Comb., The Combustion Institute, pp. 719–729.

Nieckele, A.O., Naccache, M.F., Gomes, M.S.P., Carneiro, J.E. and Serfaty, R., 2001. "Evaluation of models for combustion processes in a cylindrical furnace", ASME-IMECE, Int. Conf. of Mechanical Engineering, New York.

Nieckele, A.O., Naccache, M. F., Gomes, M.S.P., Carneiro, J.E. and Serfaty, R., 2002. "Predição da combustão de gás natural em uma fornalha utilizando reação em uma e duas etapas", CONEM – João Pessoa – PB.

Nikuradse, J., 1933. "Strömusgsgesetze in Rauhen Rohren", Forsch. Arb. Ing. – Ees.

Siegel, R. and Howell, J. R., 2002. "Thermal Radiation Heat Transfer", 4th ed., Taylor & Francis, New York - London.

Sika, P., 1991. "Evaluation of direct-exchange areas for a cylindrical enclosure", ASME T- JHT Vol. 113, pp. 1040–1044.

Smith, T., Shen, F. and Friedman, N, 1982. "Evaluation of coefficients for the WSGGM", ASME Trans -JHT 104: 602–608.

Spalding, D.B., 1979. "Combustion and Mass Transfer", Pergamon Press, Inc., New York.

Turns, S. T., 2000. An Introduction to Combustion - Concepts and Applications, 2nd edn, McGraw-Hill, New York.

Van Wylen, G. J., Sonntag, E. R. and Bornake, C., 1998. Fundamentos da Termodinâmica, 5nd ed, Edgard Blücher Ltda.

Zhou, L. X., Qiao, L., Chen, X. L. and Zhang, J., 2002. "A USM turbulence-chemistry model for simulating NOx formation in turbulent combustion", Fuel 81: 1703–1709.

10. Responsibility notice

The authors are the only responsible for the material included in his paper.